

## Structural studies of the primary donor cation radical $P_{870}^+$ in reaction centers of *Rhodospirillum rubrum* by electron–nuclear double resonance in solution

(photosynthesis/primary process/bacteriochlorophyll/special pair geometry)

W. LUBITZ\*, F. LENDZIAN†, H. SCHEER‡, J. GOTTSTEIN‡, M. PLATO†, AND K. MÖBIUS†

\*Institut für Organische Chemie, Freie Universität Berlin, Takustrasse 3, D-1000 Berlin 33; †Institut für Molekülphysik, Freie Universität Berlin, Arnimallee 14, D-1000 Berlin 33; and ‡Botanisches Institut, Universität München, Menzinger Strasse 67, D-8000 München 19, Federal Republic of Germany

Communicated by Joseph J. Katz, September 1, 1983

**ABSTRACT** The light-induced cation radical of the primary electron donor,  $P_{870}^+$ , in photosynthetic reaction centers from *Rhodospirillum rubrum* G-9, has been investigated by electron–nuclear double resonance (ENDOR) in liquid aqueous solution. The measured hyperfine coupling constants are assigned to specific molecular positions by partial deuteration. Comparison with the bacteriochlorophyll a cation radical shows different reduction factors of the individual coupling constants deviating from the value 2.0 reported in earlier investigations in frozen solutions. The average of the coupling constants is, however, reduced by a factor very close to 2.0. EPR simulations using the ENDOR coupling constants support a dimer model for  $P_{870}^+$  with  $C_2$  symmetry, where the two macrocycles are close enough to form a supermolecular orbital resulting in a different distribution of the unpaired electron, compared with the monomeric bacteriochlorophyll a cation radical. Molecular orbital calculations were used to obtain structural information about this dimer.

In bacterial photosynthesis, the light-induced charge separation starts with the fast donation of an electron from an excited singlet primary donor P to an electron-transport chain in the reaction center protein (RC) (1–5). RCs offer a convenient system for the investigation of the cation and anion radicals formed in this process.

Much of our present knowledge about the various species and their interactions in RCs has evolved from the application of paramagnetic resonance methods (3, 6). The dimeric nature of the primary donor cation radical  $P_{870}^+$  in some bacteria was originally proposed by Norris *et al.* (7) to explain the observed narrowing of the EPR line by a reduction factor (RF) of  $\sqrt{2}$  compared with the monomeric bacteriochlorophyll a cation radical (BChl-a<sup>+</sup>) (Fig. 1). Further support for this model came from electron–nuclear double resonance (ENDOR) at low temperatures in which a reduction of the hyperfine coupling constants (hfcs) by a factor of two was deduced when going from BChl-a<sup>+</sup> to  $P_{870}^+$  (8–14). The detailed structure of the suggested dimer is still controversial (3, 4, 14), but its geometry is of prime importance for basic understanding of the primary act of light-induced charge separation in photosynthesis.

ENDOR in solution has been used to elucidate the electronic structure of the various isolated pigment radicals and has provided an almost complete set of isotropic hfcs (15–20). Liquid-state ENDOR is superior to frozen-solution ENDOR (10, 21, 22) because the linewidths are smaller due to the absence of anisotropic broadening so that hfcs from all magnetic nuclei in the radical can often be obtained (23, 24). However, most of the ENDOR studies of photosynthesis thus far were carried out in frozen matrices (8–13). An EN-

DOR in solution study on RC [*Rhodospseudomonas (Rp.) sphaeroides* R-26] in water at room temperature has been reported only recently (25). In those experiments, the additional application of electron–nuclear–nuclear triple resonance (26) proved to be useful for increasing the ENDOR intensity and resolution and for determining the signs of the hfcs. This study is now extended to another bacterium—i.e., *Rhodospirillum (Rs.) rubrum* G-9.

### MATERIALS AND METHODS

*Rs. rubrum* G-9 was grown anaerobically in Hutner medium (27) at 25–32°C. After freezing and thawing, the cells were incubated for 2 hr at 25°C with lysozyme [2.5 mg/g (wet weight) of bacteria; Boehringer, Darmstadt] and EDTA (10 mM; Merck, Darmstadt), sonicated (three 1-min periods; Branson) and centrifuged for 30 min at 12,000 × g. The supernatant was then centrifuged for 1.5 hr at 55,000 × g, and the chromatophore pellet without the hard core was suspended in Tris buffer to  $A_{870} = 50$ . One method for the isolation of RCs followed essentially the procedure of Snozzi and Bachofen (28). In other preparations, the crude RCs were purified on DEAE-cellulose (DE 52, Whatman) with Tris buffer containing 0.02% lauryldimethylamine oxide instead of Triton X-100. Lauryldimethylamine oxide exchange against Triton X-100 was done after chemical reduction of the detergent to the amine (29) on a DEAE-cellulose column. The RCs were dialyzed against the same buffer after elution with 0.3 M NaCl. Ubiquinone removal was carried out by the method of Okamura *et al.* (30).

RC solutions with  $A_{870} < 3$  ( $c < 25 \mu\text{M}$ ) were first concentrated on DEAE-cellulose and then further by membrane filtration (Millipore, type PSED 25,000, 13-mm diameter) to  $c \approx 250 \mu\text{M}$ . This solution was centrifuged for 20 min at 12,000 × g and decanted from an eventually appearing greyish pellet, and 50  $\mu\text{l}$  of the resulting solution was placed under argon in the ENDOR tube (~1 mm i.d.). BChl-a esterified with geranylgeraniol (BChl-a<sub>gg</sub>) was isolated according to Strain and Svec (31). The cation radical was prepared by iodine oxidation (5 molar excess) in  $\text{CH}_2\text{Cl}_2/\text{CH}_3\text{OH}$ , 6:1 (vol/vol) under high vacuum conditions (32). The starting concentration of BChl-a was 0.1 mM; for the ENDOR measurements the radical solution was usually concentrated by a factor of ca. 3. The stability of samples prepared in this manner was up to 1 month.

ENDOR and triple resonance measurements were carried out on a laboratory-built spectrometer (23, 26, 32). *In situ* illumination of the sample in the spectral range 450–900 nm

Abbreviations: BChl-a, bacteriochlorophyll a; BChl-a<sub>gg</sub> and BChl-a<sub>p</sub>, geranylgeranyl and phytyl esters, respectively, of BChl-a; RC, reaction center; hfc, hyperfine coupling constant; hfcs, hyperfine structure; ENDOR, electron–nuclear double resonance; RF, reduction factor.

The publication costs of this article were defrayed in part by page charge payment. This article must therefore be hereby marked "advertisement" in accordance with 18 U.S.C. §1734 solely to indicate this fact.

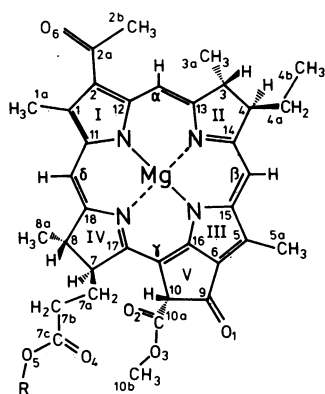


FIG. 1. Molecular structure of BChl-a with numbering scheme; R = geranylgeranyl (BChl-a<sub>gg</sub>) in *Rs. rubrum* and phytol (BChl-a<sub>p</sub>) in *Rp. sphaeroides*.

was by a tungsten/halogen lamp (250 W). The temperature stability of the sample was within  $\pm 1^\circ\text{C}$ .

## RESULTS AND DISCUSSION

**ENDOR/Triple Resonance Study of BChl-a<sup>+</sup>.** From BChl-a<sub>gg</sub> cation radical, a highly resolved ENDOR spectrum was obtained in solution, revealing 11 proton and all four <sup>14</sup>N hfc's (24, 32). The best intensity and resolution in the proton region (Fig. 2a) were achieved by special triple resonance (23). By combined use of sign determination of hfc's through general triple resonance (23), temperature-dependent nuclear relaxation studies (18, 19, 33), and deuterium labeling and exchange experiments (32), all 11 H hfc's were assigned to specific groups of  $\alpha$ - (directly attached to the  $\pi$ -system) and

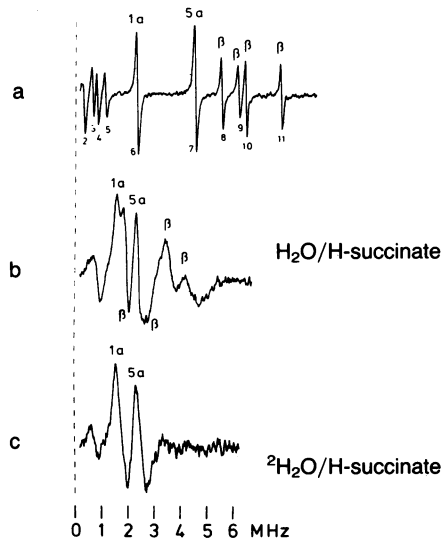


FIG. 2. Proton special triple resonance spectra of BChl-a<sub>gg</sub><sup>+</sup> [iodine oxidation in CH<sub>2</sub>Cl<sub>2</sub>/CH<sub>3</sub>OH (6:1)] (a) and of fully protonated (b) and partially deuterated in <sup>2</sup>H<sub>2</sub>O (c) P<sub>870</sub><sup>+</sup> (light-induced in RCs of *Rs. rubrum* G-9). Experimental conditions were as follows. (a) T =  $-18^\circ\text{C}$ ; microwave (mw) power, 20 mW; total rf power, 150 W; FM (10 kHz) of rf field, depth  $\pm 30$  kHz; time constant, 1 s; total averaging time, 35 min; proton hfc's (MHz) and assignments (Fig. 1) obtained: methines ( $\alpha$ ,  $\beta$ ,  $\delta$ ),  $-0.15$ ,  $+1.30$ , and  $+2.30$ ; methyls,  $+4.85$  (1a) and  $+9.50$  (5a);  $\beta$ -protons (3, 4, 7, 8),  $+11.61$ ,  $+13.00$ ,  $+13.59$ , and  $+16.43$ ; acetyl (2b),  $-0.50$ ; position 10,  $-1.65$ ; nitrogen hfc's (MHz),  $-3.17$ ,  $-3.05$ ,  $-2.35$ , and  $\pm 0.45$  (32). The symbols " $\beta$ " in this figure denote the hfc's at positions 3, 4, 7, and 8. (b and c) T =  $20^\circ\text{C}$ ; mw power, 80 mW; total rf power, 200 W; FM (10 kHz) depth  $\pm 60$  kHz; time constant, 1 s; total averaging time, 25 min. The frequency scale corresponds to one-half the coupling constant (23, 26).

$\beta$ - (one bond away from the  $\pi$ -system) protons (Fig. 2). The possibility of additional couplings from  $\gamma$ -protons in the region of the small hfc's could, however, not be rigorously excluded. The hfc's reported here for the cation radical of BChl-a<sub>gg</sub> (extracted from *Rs. rubrum*) are identical to those of BChl-a esterified with phytol (BChl-a<sub>p</sub><sup>+</sup>) (from *Rp. sphaeroides*) within experimental error ( $\leq 10$  kHz). Our hfc's are in good agreement with the seven couplings resolved by Borg *et al.* (15). Large  $\pi$ -spin densities are obtained for positions 1, 5, 13, 14, 17, and 18 (Fig. 1). Small or even negative values are found for the methine positions, the keto carbons, and all four nitrogens. This experimental result is in agreement with those from advanced MO calculations (34).

**ENDOR/Triple Resonance Study of P<sub>870</sub><sup>+</sup> in Solution.** In liquid solution, a considerable increase of spectral resolution can be achieved only if the rotational tumbling of the RC is fast enough to effectively average out the anisotropic hyperfine components. By assuming a molecular weight of  $\approx 100,000$  for the RC protein including part of the detergent shell (4, 5), a rotational correlation time ( $\tau_R$ ) of  $\approx 30$  ns in water at  $25^\circ\text{C}$  is estimated (25, 35). Thus, the Redfield condition (36) for fast motion [ $(\langle \mathcal{H}_1(t) \rangle)(\tau_R/\hbar) \ll 1$ ] is valid for nuclei having anisotropic hyperfine tensor components  $A_{ij} \leq 5$  MHz (25). Since all of the major proton hfc's in P<sub>870</sub><sup>+</sup> are expected to be of the  $\beta$ -type (methyl groups 1a and 5a, protons at positions 3, 4, 7, and 8), one can assume that for these nuclei no anisotropic broadening should be present. However, the estimated  $\tau_R$  is too large for obtaining optimum <sup>1</sup>H ENDOR signals (33) ( $\tau_R^{\text{opt}} \sim 0.1$ – $1.0$  ns). Unfortunately, for the RCs  $\tau_R$  cannot be shortened because of protein denaturation at temperatures above  $35^\circ\text{C}$ . This prevents optimization of ENDOR intensity and linewidth for RCs.

A better resolution and intensity was achieved in the special triple resonance experiment (Fig. 2b). Five lines are clearly resolved and both the second and third line show shoulders (Table 1). The signs of the seven hfc's were determined by general triple resonance. They are all positive, indicating that all these couplings belong to  $\beta$ -protons (26). Furthermore, it could be shown by the same technique that all lines in the spectrum originate from one species. The optical, EPR, and ENDOR/triple resonance spectra of chemically oxidized RCs were identical to those observed by illumination.

Assignment of the hfc's to specific groups of protons in the system was achieved by studying P<sub>870</sub><sup>+</sup> in partially deuterated RCs. In BChl-a<sub>gg</sub> extracted from bacteria grown in <sup>2</sup>H<sub>2</sub>O (99.9%)/[<sup>1</sup>H]succinic acid abundant protons are found only at positions 1a, 5a, and 2b (methyl groups; Fig. 1) and in positions more than one bond away from the  $\pi$ -system. Positions 3, 4, 7, and 8 and the methine bridges are almost completely deuterated (37). A special triple resonance spectrum obtained from partially deuterated P<sub>870</sub><sup>+</sup> is shown in Fig. 2c, and it has only two prominent lines. They are assigned to the

Table 1. Comparison of isotropic hfc's of the cation radicals of BChl-a<sub>gg</sub> and P<sub>870</sub> in RCs from *Rs. rubrum* G-9

Position (assignment)*	Hfc, MHz		
	BChl-a <sub>gg</sub> <sup>+</sup>	P <sub>870</sub> <sup>+</sup> †	RF‡
CH <sub>3</sub> (1a)	+4.85	+3.40	1.43
CH <sub>3</sub> (5a)	+9.50	+4.85	1.96
$\beta$ -H	+11.61	+3.95	2.94
$\beta$ -H } rings	+13.00	+5.28	2.46
$\beta$ -H } II, IV	+13.59	+7.50	1.81
$\beta$ -H	+16.43	+8.50	1.93

\*Compare Fig. 1; the individual assignments of the methyl protons to positions 1a and 5a are discussed in refs. 10, 11, and 13.

†ENDOR data,  $-18^\circ\text{C}$ , errors =  $\pm 20$  kHz.

‡ENDOR data,  $20^\circ\text{C}$ , errors =  $\pm 40$  kHz.

§Defined as hfc's a(BChl-a<sup>+</sup>)/a(P<sub>870</sub><sup>+</sup>).

methyl groups in positions 1a and 5a. There are only two hfc's for these methyl groups: the triple resonance lines show no tendency to split. If we assume a dimer for  $P_{870}^+$ , this finding suggests a symmetric spin distribution over both halves—i.e., protons at corresponding positions in both halves of the dimer exhibit the same hfc's. Four lines are missing as compared with Fig. 2b. They should therefore belong to the four  $\beta$ -protons (Fig. 2b) in the hydrated rings II and IV (positions 3, 4, 7, and 8; Fig. 1). Assignment of the smallest hfc in Fig. 2b and c is not so straightforward and will be discussed below.

**Dimeric Nature of  $P_{870}^+$ .** Because there are independent assignments of the measured hfc's to molecular positions for both BChl- $a^{+}$  and  $P_{870}^+$ , we can compare the spectra of those two radicals by assuming that the ordering within one group of hfc's with regard to magnitude is retained. In  $P_{870}^+$  all hfc's are reduced in magnitude as compared with BChl- $a^{+}$  but not by a constant RF of 2 (Table 1), as expected in the simplest "special pair" model (7–13). The average RF factor is nonetheless very close to 2 (2.06), still indicating a dimeric structure of  $P_{870}^+$ . The procedure of comparing hfc's is, however, questionable because of the uncertain relationship between hfc's and spin densities [dihedral angles of the  $\beta$ -protons (38), shifting of spin density to "blind" positions].

An independent approach to confirm the dimeric nature of  $P_{870}^+$  is to simulate the EPR spectrum by using the observed ENDOR hfc's (Fig. 3). In case a, we have assumed a dimer, in case b, a monomer. The EPR spectrum of  $P_{870}^+$  in *Rs. rubrum* is only compatible with a dimer of BChl- $a_{88}$  molecules, provided all relevant hfc's have been observed in the ENDOR spectrum (see below). This conclusion is in accordance with recent EPR results of Wasielewski *et al.* (39) based on a second-moment analysis of  $^2\text{H}$ - and  $^{13}\text{C}$ -enriched  $P_{870}^+$  and BChl- $a^{+}$ .

**ENDOR/Triple Resonance Study of  $P_{870}^+$  at Lower Temperatures.** The reduction factors presented in Table 1 are at variance with earlier solid-state ENDOR studies (9, 12) reporting a halving of all observed individual hfc's. To clarify this discrepancy, we have studied  $P_{870}^+$  in RCs in  $\text{H}_2\text{O}/\text{glycerol}$ , 1:1 (vol/vol) at different temperatures (Fig. 4). In this viscous solution, anisotropic line broadening occurs at room temperature and becomes very pronounced at somewhat lower temperatures. At  $4^\circ\text{C}$  the resonances of the methyl groups (1a, 5a) have merged to one slightly split line (Fig. 4c). In contrast to an earlier assignment (9, 12), both methyl groups therefore belong to line 2 and not to lines 1 and 2,

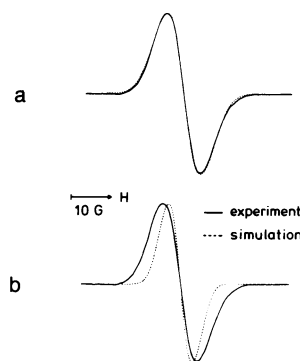


FIG. 3. Experimental (—) and simulated (---) EPR spectra of light-induced  $P_{870}^+$  in RCs of *Rs. rubrum* G-9 ( $20^\circ\text{C}$ ). The data and assignments from Table 1 were used for the simulations. (a) Simulation by assuming a dimer (twice the number of protons belonging to each hfc); basic linewidth, 2.3 G. (b) Simulation by assuming a monomer; basic linewidth 3.2 G ( $\sqrt{2} \times 2.3$  G). The basic linewidth for the dimer simulation was obtained from the residual small hfc's in  $P_{870}^+$  ( $2 \times$  three protons) and from the  $^{14}\text{N}$  couplings in BChl- $a^{+}$  (Fig. 2), each hfc halved and assigned to two  $^{14}\text{N}$  nuclei.

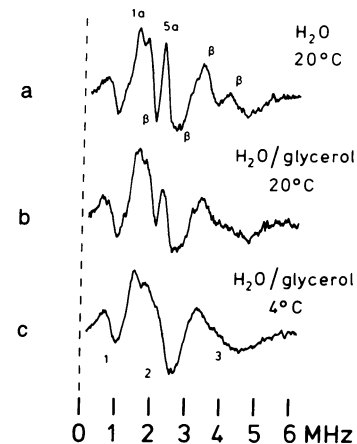


FIG. 4. Proton special triple resonance spectra of  $P_{870}^+$  in RCs of *Rs. rubrum* G-9 in water and water/glycerol, 1:1 (vol/vol) at different temperatures. See Fig. 2 for other experimental conditions. Hfc values at low temperature ( $-130^\circ\text{C}$ ) are 1.4 (line 1), 4.5 (line 2), and 7.8 (line 3) MHz. Norris *et al.* (6) reported values of 0.8, 2.2, 4.7, and 7.0 MHz for chemically oxidized whole cells at  $-173^\circ\text{C}$ .

respectively. Furthermore, only two out of the four  $\beta$ -protons belong to line 3; the others are masked by the strong methyl resonances.

The spectra shown in Fig. 4 have been followed down to  $-150^\circ\text{C}$  where no further changes occurred. The hfc's obtained at low temperatures are in fair agreement with earlier results (6, 12). The line broadening observed is fully reversible and can be attributed to nonaveraged hyperfine anisotropy (21, 22).

**Discussion of the  $P_{870}^+$  Hyperfine Structure (hfs) Data.** In contrast to the methyl hfc's (Table 1)—which directly reflect the spin density at the adjacent carbon centers—the  $\beta$ -proton couplings at positions 3, 4, 7, and 8 are strongly influenced by the geometries of the flexible rings II and IV (38). These can be either twisted or tilted with respect to the molecular plane (ref. 40 and p. 505 of ref. 41). A change in the twist or tilt angle of  $\approx 10^\circ$  or  $20^\circ$ , respectively, is sufficient to account for the observed RFs of the  $\beta$ -proton hfc's assuming a halving of the adjacent  $\pi$ -carbon spin densities. A decision about the relative contributions of the tilt and twist angles and of possible  $\pi$ -spin density shifts (as observed for the methyl groups, Table 1) is difficult to make because the hfc's of these  $\beta$ -protons cannot be individually assigned.

Another complication arises from the residual small positive hfc ( $a = +1.60$  MHz). It is present in the triple resonance spectrum of  $P_{870}^+$  (Fig. 2b), and persists in the deuterated species (Fig. 2c). Regarding the isotopic distribution of the selectively deuterated species (37), one would attribute this coupling to position 2b (acetyl group) (Fig. 1). Comparison with BChl- $a^{+}$  ( $a_{2b} = -0.5$  MHz) implies a significant change in magnitude and sign of this hfc. This may, however, be possible if the acetyl group geometry is changed. Another possible assignment would be to  $\gamma$ -protons in rings II and/or IV, which are also partially protonated in the deuterated species. No such resonances were detected in BChl- $a^{+}$ , although a superposition in the range of the small hfc's ( $\approx 0.5$  MHz) cannot be rigorously excluded. Furthermore, such an assignment implies a change of the angles of rings II and/or IV, which—in this case—must result in a considerable increase in the  $\gamma$ -proton hfc's. The third possibility involves interactions with sufficiently close protons of proteins, which might participate in the formation and the linkage of the BChl dimer (42, 43).

So far, no  $^{14}\text{N}$  ENDOR has been detected in  $P_{870}^+$ . This might be explained by the larger hfs anisotropy of this nucleus, which renders the detection more infeasible (33) at the

given  $\tau_R$  of  $\approx 30$  ns. Further complications may arise from the nonaveraged  $^{14}\text{N}$  quadrupole interaction.

Comparison between the hfs data for  $\text{P}_{870}^{+\cdot}$  in *Rs. rubrum* G-9 and those obtained in *Rp. sphaeroides* R-26 (25) leads to similar conclusions about the dimeric nature of  $\text{P}_{870}^{+\cdot}$  in the latter bacterium (32). The measured hfs data are, however, persistently different for the two species, irrespective of the preparation procedure. Because we could not detect any differences between the hfs of the isolated BChl-a cation radicals bearing different side chains (phytyl or geranylgeranyl), this observation should be attributed to an altered protein environment in the RCs that forces the pigments to form a slightly different dimer (2). Another possibility involves a different anchoring of the molecules by these side chains in the hydrophobic environment (42, 43).

**Structural Proposal for  $\text{P}_{870}^{+\cdot}$ .** The hfs data not only support the dimeric nature of  $\text{P}_{870}^{+\cdot}$  but also contain information about the geometry of the two molecules. A proposed model must be able to account for the following experimental observations. (i) The halves of the dimer are equivalent with respect to their hfs; i.e., they are related by a  $C_2$ -symmetry axis. (ii) Corresponding  $\pi$ -spin densities in both halves are not scaled down by a constant factor of 2 but rather exhibit different individual RFs. On the basis of these findings an asymmetric dimer—e.g. with nonparallel planes (42, 43)—is quite unlikely. The observed spin distribution can be explained by delocalization (44) over a symmetric dimer, in which the unpaired electron occupies a "super molecular orbital" extending over both halves. The interplanar distance of the two halves must be equal to or less than the van der Waals distance of aromatic  $\pi$ -systems, to provide sufficient orbital overlap for spin delocalization. The model proposed by Fong (45) does not meet this requirement. The only dimer model already existing in the literature that fulfills the above requirements has been proposed by Shipman *et al.* (46) and by Boxer and Closs (47) for a chlorophyll a dimer. On the basis of NMR data obtained from covalently or coordinatively (48) linked BChl molecules, Wasielewski *et al.* (49) proposed a similar model for the bacterial primary donor. To test whether our experimental observations can be explained in the framework of this model, we have carried out a series of simple Hückel MO calculations [modified complete neglect of differential overlap parametrization (50), geometrical data: keto group at ring III from ref. 51, otherwise standard bond lengths and angles] on a dimer constructed from the  $\pi$ -skeletons of the two macrocycles, including the keto groups at rings I and III (Fig. 5). A test calculation on the cation radical of one—monomeric—half yielded a spin-density distribution (Table 2) that, although not very satisfactory in absolute numbers, agrees sufficiently well with the experimental results. A particular success is the correct prediction of the observed ratio of  $\approx 1:2$  of the spin densities at  $C_1$  and  $C_5$  as a consequence of the distorted geometry of the keto group  $C_9-O_1$  (51). Our conclusions concerning the dimer model are based on ratios of large positive spin densities (mainly 1- and 5- $\text{CH}_3$ ) for which inherent deficiencies of the Hückel method should be less important.

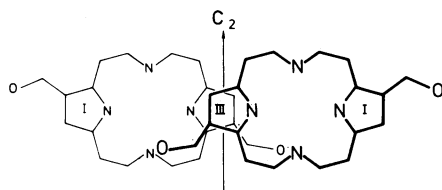


FIG. 5. Dimer model for  $\text{P}_{870}^{+\cdot}$  constructed from the  $\pi$ -skeletons of two BChl-a molecules. The geometrical arrangement corresponds to an optimum agreement between the experiments and the Hückel MO calculations.

Table 2. Theoretical  $\pi$ -spin densities  $\rho_c^\pi$  of a radical cation for a monomeric and dimeric model of BChl-a (for numbering of positions, see Fig. 1)

Position	Monomer*	Dimer†	
		A	B
$C_1$	0.074	0.042 (1.76)	0.045 (1.61)
$C_5$	0.137	0.063 (2.17)	0.053 (2.58)
$C_{13}$	0.071	0.037 (1.92)	0.042 (1.69)
$C_{14}$	0.084	0.041 (2.05)	0.043 (1.95)
$C_{17}$	0.074	0.033 (2.24)	0.040 (1.85)
$C_{18}$	0.082	0.039 (2.10)	0.045 (1.82)

Spin densities for methine and  $^{14}\text{N}$  positions are omitted because of their small magnitudes.

\*Isotropic hfs can be obtained from  $\rho_c^\pi$  by use of appropriate  $Q$  factors (52).

†Numbers in parentheses represent RFs:  $\rho_c^\pi$  (monomer)/ $\rho_c^\pi$  (dimer). Distance of planes, 3.0 Å; horizontal shift, 7.0 Å (A) or 8.0 Å (B) (see Fig. 5).

The resulting dimer geometry (Fig. 5), which is similar to models proposed earlier (46, 47, 49), is characterized as follows. (i) The equivalence of the two halves of the dimer is assured by adopting a model with  $C_2$  symmetry. A tilt angle of only  $5^\circ$  between the two planes results in a 25% inequivalence of spin densities at corresponding positions. The two halves may, however, be rotated relative to each other around an axis perpendicular to the monomer planes. This produces relatively small shifts in the individual  $\pi$ -spin densities without loss of the pair equivalence and can therefore not be excluded. (ii) A distance of 3–3.5 Å of the planes must be used to obtain shifts in the spin densities similar to those observed in the ENDOR spectra (Tables 1 and 2). (iii) Maximum overlap in the region of ring III results in a stronger reduction of the spin density at position 5 than at position 1, which is experimentally observed (Table 1).

Our MO calculations are at present preliminary because only  $\pi$ -orbitals have been considered. However, extended Hückel calculations using an all-valence-orbital basis set have shown that  $\pi$ - $\sigma$  separation appears to be a good approximation for distances of the planes  $\geq 2.5$  Å.

An alternative explanation for the observed reduction of large proton couplings in  $\text{P}_{870}^{+\cdot}$  is that there may be an efficient mixing of the ground state  $D_0$  and first excited doublet state  $D_1$  of a BChl-a $^{+\cdot}$  monomer in the RC on account of the protein environment. The methyl- and  $\beta$ -proton couplings are predicted to be considerably smaller in  $D_1$  than in  $D_0$  (34, 53, 54). However, mechanisms of this type also predict that the hfs for the methine protons, for  $^{14}\text{N}$ , and for the  $\beta$ -proton in ring V (position 10) will lie in a frequency range in which they should be detectable by ENDOR—in contrast to the predictions of the dimer model. None of these predicted lines has been observed in our ENDOR experiments, but further work is necessary for an unequivocal decision. The detection of the methine proton and  $^{14}\text{N}/^{15}\text{N}$  hfs would be of particular interest. The most promising results are anticipated from single-crystal-type ENDOR spectra. These may be obtained by studying either RC single crystals (55) or by orientational selection in EPR powder spectra (21) via the increased separation of the g tensor principal components in higher magnetic fields (56).

The skillful technical assistance of C. Bubenzer (München) is gratefully acknowledged. This work was supported by Sfb 161 (Berlin) and 143 (München) from the Deutsche Forschungsgemeinschaft.

1. Clayton, R. K. (1980) *Photosynthesis: Physical Mechanisms and Chemical Patterns* (Cambridge Univ. Press, London).
2. Okamura, M. Y., Feher, G. & Nelson, N. (1982) in *Photosynthesis: Energy Conversion by Plants and Bacteria*, Vol. 1, ed. Govindjee (Academic, New York) pp.195–272.

3. Hoff, A. J. (1982) in *Light Reaction Path of Photosynthesis*, ed. Fong, F. K. (Springer, Berlin), pp. 80–151; and 322–326.
4. Feher, G. & Okamura, M. Y. (1978) in *The Photosynthetic Bacteria*, eds. Clayton, R. K. & Sistrom, W. R. (Plenum, New York), pp. 349–386.
5. Gingras, G. in *The Photosynthetic Bacteria*, eds. Clayton, R. K. & Sistrom, W. R. (Plenum, New York), pp. 119–132.
6. Norris, J. R., Scheer, H. & Katz, J. J. (1979) in *The Porphyrins*, ed. Dolphin, D. (Academic, New York), Vol. 4, pp. 159–195.
7. Norris, J. R., Uphaus, R. A., Crespi, H. L. & Katz, J. J. (1971) *Proc. Natl. Acad. Sci. USA* **68**, 625–629.
8. Norris, J. R., Druyan, M. E. & Katz, J. J. (1973) *J. Am. Chem. Soc.* **95**, 1680–1682.
9. Feher, G., Hoff, A. J., Isaacson, R. A. & McElroy, J. D. (1973) *Biophys. J.* **13**, 61 (abstr.).
10. Feher, G., Hoff, A. J., Isaacson, R. A. & Ackerson, L. C. (1975) *Ann. N.Y. Acad. Sci.* **244**, 239–259.
11. Norris, J. R., Scheer, H. & Katz, J. J. (1975) *Ann. N.Y. Acad. Sci.* **244**, 260–280.
12. Norris, J. R., Scheer, H., Druyan, M. E. & Katz, J. J. (1974) *Proc. Natl. Acad. Sci. USA* **71**, 4897–4900.
13. Norris, J. R. & Katz, J. J. (1978) in *The Photosynthetic Bacteria*, eds. Clayton, R. K. & Sistrom, W. R. (Plenum, New York), pp. 397–418.
14. Parson, W. W. (1982) *Annu. Rev. Biophys. Bioeng.* **11**, 57–80.
15. Borg, C. D., Forman, A. & Fajer, J. (1976) *J. Am. Chem. Soc.* **98**, 6889–6893.
16. Fajer, J., Forman, A., Davis, M. S., Spaulding, L. D., Brune, D. C. & Felton, R. H. (1977) *J. Am. Chem. Soc.* **99**, 4134–4140.
17. Hoff, A. J. & Möbius, K. (1978) *Proc. Natl. Acad. Sci. USA* **75**, 2296–2300.
18. Lubitz, W., Lendzian, F. & Möbius, K. (1981) *Chem. Phys. Lett.* **81**, 235–241.
19. Lubitz, W., Lendzian, F. & Möbius, K. (1981) *Chem. Phys. Lett.* **84**, 33–38.
20. Lendzian, F., Lubitz, W. & Möbius, K. (1982) *Chem. Phys. Lett.* **90**, 375–381.
21. Kevan, L. & Kispert, L. D. (1976) *Electron Spin Double Resonance Spectroscopy* (Wiley, New York), pp. 233–253.
22. Hyde, J. S., Rist, G. H. & Eriksson, L. E. G. (1968) *J. Phys. Chem.* **72**, 4269–4275.
23. Möbius, K., Plato, M. & Lubitz, W. (1982) *Phys. Rep.* **82**, 171–208.
24. Möbius, K., Fröhling, W., Lendzian, F., Lubitz, W., Plato, M. & Winscom, C. J. (1982) *J. Phys. Chem.* **86**, 4491–4507.
25. Lendzian, F., Lubitz, W., Scheer, H., Bubenzer, C. & Möbius, K. (1981) *J. Am. Chem. Soc.* **103**, 4635–4637.
26. Möbius, K. & Biehl, R. (1979) in *Multiple Electron Resonance Spectroscopy*, eds. Dorio, M. M. & Freed, J. H. (Plenum, New York), pp. 475–507.
27. Cohen-Bazire, G., Sistrom, W. R. & Stanier, J. (1957) *J. Cell. Comp. Physiol.* **49**, 25–68.
28. Snozzi, M. & Bachofen, R. (1979) *Biochim. Biophys. Acta* **546**, 236–247.
29. Pachence, J., Dutton, P. L. & Blasié, J. K. (1979) *Biochim. Biophys. Acta* **548**, 348–373.
30. Okamura, M. Y., Isaacson, R. A. & Feher, G. (1975) *Proc. Natl. Acad. Sci. USA* **72**, 3491–3495.
31. Strain, H. H. & Svec, W. A. (1966) in *The Chlorophylls*, eds. Vernon, L. P. & Seely, G. R. (Academic, New York).
32. Lendzian, F. (1982) Dissertation (Freie Universität, Berlin, Federal Republic of Germany).
33. Plato, M., Lubitz, W. & Möbius, K. (1981) *J. Phys. Chem.* **85**, 1202–1219.
34. Petke, J. D., Maggiora, G. M., Shipman, L. L. & Christoffer-son, R. E. (1980) *Photochem. Photobiol.* **31**, 243–257.
35. Chasteen, N. D. & Francavilla, J. (1976) *J. Phys. Chem.* **80**, 867–871.
36. Redfield, A. G. (1965) *Adv. Magn. Reson.* **1**, 1–32.
37. Katz, J. J., Dougherty, R. C., Crespi, H. L. & Strain, H. H. (1966) *J. Am. Chem. Soc.* **88**, 2856–2857.
38. Davis, M. S., Forman, A., Hanson, L. K., Thornber, J. P. & Fajer, J. (1979) *J. Phys. Chem.* **83**, 3325–3332.
39. Wasielewski, M. R., Norris, J. R., Crespi, H. L. & Harper, J. (1981) *J. Am. Chem. Soc.* **103**, 7664–7665.
40. Chow, H. C., Serlin, R. & Strouse, C. E. (1975) *J. Am. Chem. Soc.* **97**, 7230–7237.
41. Scheer, H. & Katz, J. J. (1975) in *Porphyrins and Metalloporphyrins*, ed. Smith, K. M. (Elsevier, New York), pp. 399–524.
42. Schaafsma, T. J. (1982) in *Triplet State ODMR Spectroscopy*, ed. Clarke, R. H. (Wiley, New York), pp. 291–365.
43. Hoff, A. J. (1982) in *Triplet State ODMR Spectroscopy*, ed. Clarke, R. H. (Wiley, New York), pp. 367–425.
44. Bowman, M. K. & Norris, J. R. (1982) *J. Am. Chem. Soc.* **104**, 1512–1515.
45. Fong, F. K. (1974) *Proc. Natl. Acad. Sci. USA* **71**, 3692–3695.
46. Shipman, L. L., Cotton, T. M., Norris, J. R. & Katz, J. J. (1976) *Proc. Natl. Acad. Sci. USA* **73**, 1791–1794.
47. Boxer, S. G. & Closs, G. L. (1976) *J. Am. Chem. Soc.* **98**, 5406–5408.
48. Cotton, T. M., Loach, P. A., Katz, J. J. & Ballschmiter, K. H. (1978) *Photochem. Photobiol.* **27**, 735–749.
49. Wasielewski, M. R., Smith, U. H., Cope, B. T. & Katz, J. J. (1977) *J. Am. Chem. Soc.* **99**, 4172–4173.
50. Pople, J. A. & Beveridge, D. L. (1970) *Approximate Molecular Orbital Theory* (McGraw-Hill, New York), pp. 75–79.
51. Barkigia, K. M., Fajer, J., Smith, K. M. & Williams, G. J. B. (1981) *J. Am. Chem. Soc.* **103**, 5890–5893.
52. Sanders, J. K. M., Newton, C. G. & Waterton, J. C. (1978) *J. Magn. Reson.* **31**, 49–53.
53. Fajer, J., Borg, D. C., Forman, A., Felton, R. H., Vegh, L. & Dolphin, D. (1973) *Ann. N.Y. Acad. Sci.* **206**, 349–364.
54. O'Malley, P. M. & Babcock, G. T. (1984) in *Proc. 6th Int. Congr. Photosynthesis*, Brussels, ed. Sybesma, C., in press [(1983) *Proc. 6th Int. Congr. Photosynthesis Abstr.* **1**, abstr. 104.1].
55. Michel, H. (1982) *J. Mol. Biol.* **158**, 567–572.
56. Grinberg, O. Ya., Dadali, A. A., Dubinskii, A. A., Vasserman, A. M., Buchachenko, A. L. & Lebedev, Ya. S. (1979) *Teoreticheskaya i Éksperimental'naya Khimiya* **15**, 583–588.